Hypsometrical Change of Gangotri Glacier since 1968 using Multitemporal DEM's

Mohd Anul Haq
Indian Institute of Technology Roorkee
Roorkee, Pin Code-247667
Uttarakhand, India

Kamal Jain, PhD.
Indian Institute of Technology Roorkee
Roorkee, Pin Code-247667
Uttarakhand, India

K. P. R. Menon, PhD.
National Remote Sensing Centre
Balanagar, Hyderabad,
Pin Code-500037, India.

ABSTRACT

Precise estimate of glaciers, directly or indirectly influence most of the glaciological studies like ice extent, terminus position, mass balance studies, etc, thus mapping of snow and ice covered areas have continuously been one of the foremost scientific goals. Difficult access and unpredictable atmospheric condition that characterize the glacier areas have created remote sensing the foremost valuable tool for comprehensive and multi temporal study of those areas during a cost effective manner. Thus remote sensing information spinning most the regions of the spectrum are oftentimes utilized for mapping of glacier regions in different parts of the world. Current investigation derived the change in Gangotri glacier extent along with elevation classes using multitemporal digital elevation models (DEM's) extracted from Corona 1968 and ASTER 2010 imagery.

General Terms

Remote Sensing, GIS, GPS

Keywords

Corona, hypsography, DEM, ASTER

1. INTRODUCTION

Monitoring of glaciers motivates scientific interest for two main reasons. First, Glaciers change monitoring has been used for climatic change investigation. The surface area and volume of individual glaciers are monitored to estimate future water availability. Second, glaciers in Indian Himalayas have been recognized as important water storage systems for municipal, industrial and hydroelectric power generation purposes. An increasing number of glaciological studies are focusing on monitoring glacier changes using remote sensing in mountain regions experiencing rapid changes in glacier extents in Himalayas [1, 2, 3, 4, 5].These studies show the potential of remote sensing data to provide useful information for glaciological applications such as: glacier area, length, surface elevation, surface flow fields, accumulation/ablation rates, albedo, equilibrium line altitude (ELA), and accumulation area ratio (AAR). [6] Calculated future glacier extent in the Swiss Alps by using hypsographic modeling. [7] Estimated ice extent and volume for the Akshiyrak Range in the interior Tien Shan of Central Asia using hypsography of ASTER imagery.

In this paper the change in ice extent with respect to elevation classes of Gangotri glacier from 1968 to 2010 using Corona and Advanced Spaceborne Thermal Emission and Reflection Radiometer (ASTER) imagery and DEM has been performed. The main objective was to derive the hypsometrical change of Gangotri glacier from 1968-2010.

2. STUDY AREA AND DATA SOURCES

Gangotri Glacier originates in the Chaukhamba massif (6853–7138 m.a.s.l.) and flows northwest towards Goumukh. The equilibrium-line altitude (ELA) of Gangotri Glacier is 4875 m a.s.l. [8], it lies between 79°4' 46.13" E-79°16' 9.45" E and 30°43' 47.00" N-30°55' 51.05" N [9]. The Gangotri glacier, one of the largest ice bodies in the Garhwal Himalayas, is located in the Uttarkashi district of the state of Uttarakhand in India (Fig. 1).

Fig 1: Snout of Gangotri glacier (Photo M Anulhaq, 14/10/2012)

Snow and glaciers contribute about 29% to the annual flows of the Ganga (up to Devprayag) and hence any impacts on these glaciers are likely to affect this large river system [10]. Gangotri glacier with TG's such as Chaturangi, Sumeru, Ghanohim, Kriti, and Miandi were analyzed in current investigation.

The Corona 1968 imagery and the multi-spectral satellite data of ASTER for 2010 have been procured in the present study (Table 1). Corona data was provided by USGS and ASTER data was provided by ECHO under the umbrella of NASA LPDAAC.

Table 1: Details of Satellite data used in the analysis

Data	Acquisition date	Spatial resolution (m)	Scene ID
Corona	27/09/1968	8	70MM X DS1048-113DA107 70MM X DS1048-113DA108 70MM X DS1048-113DA109
ASTER	29/10/2010	15,30,90	AST_L1A_003102920100529 05_20111022011841_1474 AST_L1A_003102920100529 14_20111022011841_1476.

3. METHODOLOGY

DEM was generated using Corona 1968 imagery and ASTER DEM 2010 was taken from previous investigation.

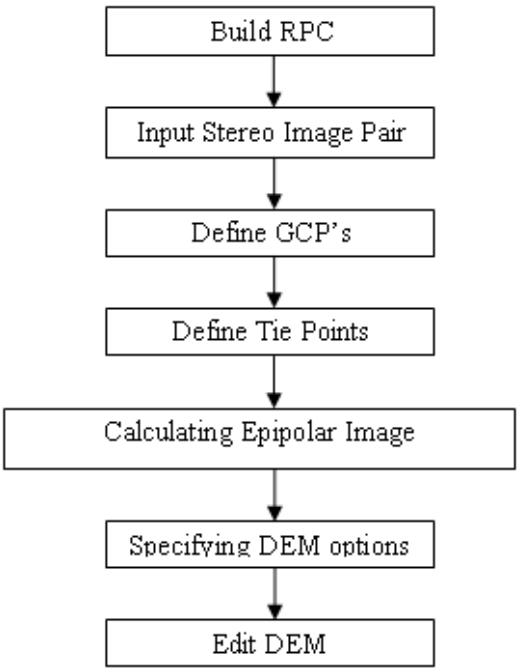

Fig 2: Methodology used in current investigation for DEM Generation

ENVI 4.8 was used for processing Corona image (1968) and DEM generation. Before generating a DTM the distortion in Corona Filmstrip has to be corrected applying a distortion factor (Kraus 1990, p. 430). Very less data specifications are known for CORONA, as shown in Table 1. The parameters 'fiducial marks' and 'principal point', which are typically used for aerial photo triangulation, does not exist. Therefore, triangulation and geometric correction becomes very difficult.

Usually, the interior orientation is defined by the help of—among others—the image parameters 'principal point' and 'fiducial marks.' However, from the CORONA camera, these parameters do not exist. Furthermore, CORONA has a panoramic camera, which produces images with high geometric deformations. Therefore, usually many steps are required to correct the image and calculate the interior orientation by removing the panoramic deformation by a mathematical algorithm, and then allocating a pseudo principal point and/or fiducial marks (relative to the ones of the whole filmstrip) to each forward- and aft-scanned image part.

A rational polynomial camera (RPC) model is a kind of generic sensor model that can be used in different remote sensing systems to model the relationship between object space and image space and transform image data to conform to a map projection [11].Usually RPC file is necessary to generate the DEM. The name "rational polynomial" derives from the fact that the model is expressed as the ratio of two cubic polynomial expressions [12]. Corona does not have RPC file so before generating DEM the RPC was generated for each 3 sets of corona imagery. RPCs are computed using a digital photogrammetry technique that uses a collinearity equation to construct sensor geometry, where the object point, perspective center, and image point are all on the same space line. The technique includes two preprocessing steps to build the sensor geometry: interior orientation (which transforms the pixel coordinate system to the camera coordinate system), and exterior orientation (which determines the position and angular orientation parameters associated with the image).

To compute RPC ENVI 4.7 was used. It requires focal length, principal point, interior orientation and exterior orientation parameters. Principal point coordinates are often set to [0.0, 0.0], which assumes that the principal point is the center of the image for a frame central projection, and the center of each scan line for a line central projection(ENVI 4.7 help menu). Principal point coordinates are often set to [0.0, 0.0], which assumes that the principal point is the center of the image for a frame central projection, and the center of each scan line for a line central projection. Principal point coordinates are often set to [0.0, 0.0], which assumes that the principal point is the center of the image for a frame central projection, and the center of each scan line for a line central projection. Focal length is the orthogonal distance from the perspective center to the image focal plane. For interior orientation parameters pixel size on the camera lens was required. Following relationship was used to find the pixel size on the camera lens;

Pixel size on the camera lens $PC = f \times GR \div H$

Where:

f is the focal length(305 mm)

H is the satellite altitude (171 km)

GR is the ground sample distance or ground resolution (7.6 m).

Interior orientation establishes the relationship between the camera model and the aerial photograph image. ENVI 4.7 uses tie points between the aerial photograph and the camera fiducial marks and the camera focal length. To compute fiducial marks the value of PC was used. Exterior orientation parameters determine the position and angular orientation associated with the aerial image. For exterior orientation 20 GPS points were used; which are well sparse around study area having accuracy of ± 5 m using Trimble Handheld GPS (See Figure 6), 50 more GCPs, measured in both stereo pair image (aft and forward) using 1999 Landsat 7 (Band) image as references for GCP measurement. The Cartosat DEM 2006 with a resolution of 30 meter was used to get the point height of the Landsat GCPs. The Build RPC dialog lists six exterior

orientation parameters (XS, YS, ZS, Omega, Phi, and Kappa), along with the units of the rotation angles, and the rotation system used. The rotation matrix associated with XS, YS, and ZS is calculated from three rotation angles: Omega, Phi, and Kappa. While the rotation angles are different among rotation systems, the rotation matrix is the same (ENVI -4.7 help).

Omega/Phi/Kappa: SX is the primary axis, defined as a fixed axis whose space direction does not change while the direction of the other axes changes as the space is rotated. Omega is a rotation about the SX axis, Phi is a rotation about the SY axis, and Kappa is a rotation about the SZ axis. The following Figure 6 shows the positive directions of all the rotation angles (ENVI 4.7 -help).

RPC was computed for 3 pairs (6 subsets), the RPC information was added to the input file header for DEM generation. Around 50 GCP's were used for exterior orientation. Additionally, 100 tie points selected in such a way that these are well spread over the common area were also used. In addition, automatically selected tie points (TPs) were used to improve the sensor models. The overall quality of the generated raw DTMs appears promising as the glacier tongues are almost fully represented. Data gaps occur mainly due to snow cover and cast shadow.

Well sparse 20 GPS points (accuracy +- 5m) taken from GPS survey in 2012 were utilized for Image to Image registration processing. We focused on the adjustment of the area around both glaciers on Corona images in respect of ASTER imagery for consistency of results during rectification of Corona imagery. We obtain the geometric relationship between the warp image and base image through 30 tie points and modeled the relationship using transformation capabilities. We mask the both DEM's (Corona DEM and ASTER DEM) using glacier outline extracted from Corona and ASTER VNIR images.

The hypsography was calculated for each glacier within the GIS in 100 m elevation bins. It has been done for the years 1968 and 2010 using the DEM divided by 100 meter zonal grid and the gridded glacier areas with a glacier-specific value as the value grid.

4. RESULTS

Earlier studies on the recession of Gangotri Glacier using topography map and satellite data show higher estimation of retreat than our assessments. For example, the present study suggests that Gangotri Glacier shrank by 5.63 km^2 (0.134 km^2 a^{-1}) between 1968 and 2010, whereas [13] claimed that it reduced by 15.5 km^2 (~0.51 km^2 a^{-1}) between 1976 and 2006, and [8] found that it reduced by 10 km^2 (0.62km^2 a^{-1}) between 1985 and 2001. The main reason for the deviation could be the debris-covered terminus of this glacier is not distinct and snout retreat is obscured. We noticed that glacier was retreat on all altitude levels but there are two elevation levels where glacier area increased very slightly; those are on the 5550 m.a.s.l. altitude the area was increased 0.123 km^2 and on 6150 altitude the area was 0.204 Km^2.

5. CONCLUSIONS

The current study provides a comprehensive multitemporal fluctuation of Gangotri Glacier from 1968 to 2010. Outlines of Gangotri glacier and digital elevation models (DEM's) were combined, both extracted from Corona Imagery of 1968 and ASTER data of 2010, to estimate change in ice extent with respect to hypsography. The results show that Gangotri glacier lost 5.63 km^2 (0.134 km^2 a^{-1}). However, the rate of retreat is less than previously estimated by toposheets and satellite imagery.

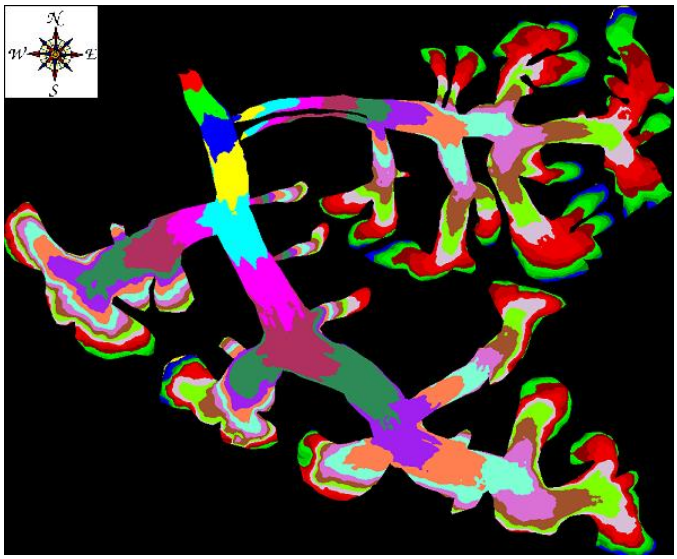

Fig 3: Hypsography of Gangotri Glacier System, 1968 at 100 (m) interval from 4050 m.a.s.l to 6050 m.a.s.l.

Due to low cost, higher resolution and historical data, the CORONA aerial imagery is especially useful for a developing country like India [14]. Due to the stereo capability CORONA photographs have the potential to generate DEMs for inaccessible areas where data from other sources are not available. ASTER may one of the most suitable sensor for monitoring of glacier parameters, with some main advantages over the other sensors include: spatial resolution of 15m in VNIR is adequate for regional-scale glacier studies and the off-nadir viewing band in the NIR enables Mid-resolution along-track stereoscopic vision and DEM generation.

6. ACKNOWLEDGEMENTS

We thank LPDAAC, NASA, and USGS for providing CORONA and ASTER data at no cost for educational research purpose.

Table 2: Area of Gangotri glacier at different elevation range

Elevation	Area in 1968(km^2)	Area in 2010(km^2)
4050	0.870	0.611
4150	1.439	1.422
4250	2.251	2.142
4350	3.439	3.422
4450	5.687	5.532
4550	6.984	6.830
4650	11.254	10.852
4750	13.980	13.41
4850	13.540	12.959
4950	15.190	14.975
5050	14.987	14.486

5150	14.660	14.061
5250	14.879	14.774
5350	14.987	14.732
5450	13.589	12.968
5550	13.000	13.123
5650	14.658	14.133
5750	12.104	11.703
5850	10.490	10.229
5950	7.879	7.747
6050	4.730	4.672
6150	2.314	2.518
6250	1.399	1.394
6350	0.560	0.556
6450	0.250	0.247
6550	0.060	0.052
Total	**215.180**	**209.550**

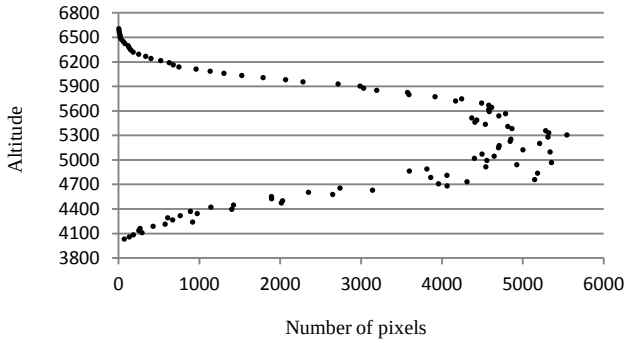

Fig 4: Scatter plot showing number of pixels at corresponding altitude (1968).

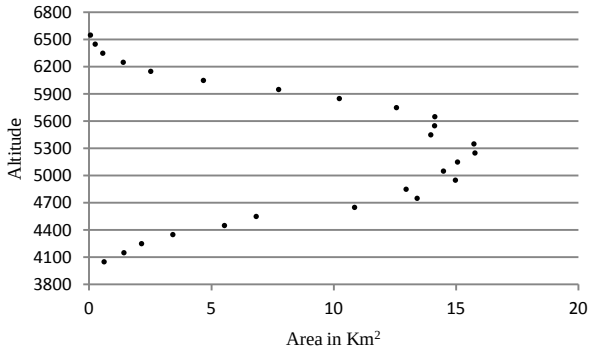

Fig 5: Scatter plot showing altitude wise Area in km^2 (1968).

7. REFERENCES

[1] Fujita, K.; Nakawo, M.; Fujii, Y.; Paudyal, P. Changes in glaciers in Hidden Valley, Mukut Himalaya, Nepal Himalayas, from 1974 to 1994. J Glaciology 1997, 43(145), 583-588.

[2] Kulkarni, A.V.; Bahuguna, I.M. Glacial retreat in the Baspa basin, Himalaya, monitored with satellite stereo data. J. Glaciology 2002, 48(160), 171-172.

[3] Bahuguna, I.M.; Kulkarni, A.V.; Nayak, S. DEM from IRS-1C PAN stereo coverages over Himalayan glaciated region - accuracy and its utility. Int Journal Remote Sensing 2004, 25(19), 4029-4041.

[4] Kulkarni, A.V.; Rathore, B.P.; Mahajan, S.; Mathur, P. Alarming retreat of Parbati glacier, Beas basin, Himachal Pradesh. Current Science 2005, 88(11), 1844-1850.

[5] Kääb, A. Combination of SRTM3 and repeat ASTER data for deriving alpine glacier flow velocities in the Bhutan Himalaya. Remote Sensing of Environment 2005, 94(4), 463-474.

[6] Paul F.,Maisch M., C.Rothenbühler, M.Hoelzle ,W. Haeberli, Calculation and visualisation of future glacier extent in the Swiss Alps by means of hypsographic - modelling, Global and Planetary Change 55 (2007) 343–357.

[7] Khalsa, S.J.S.; Dyurgerov, M.B.; Khromova, T.;Raup, B.H.; Barry, R.G. Space-based mapping of glacier changes using ASTER and GIS tools. IEEE Trans Geoscience and Remote Sensing 2004, 42(10), 2177-2183.

[8] Ahmad, S. and S.I. Hasnain. 2004. Analysis of satellite imageries for characterization of glaciomorphological features of the Gangotri Glacier, Ganga headwater, Garhwal Himalayas. Geol. Surv. India Special Publication 80, 60–67.

[9] Anulhaq M., Jain K and Menon K.P.R, "Change Detection of Himalayan Glacier Surface Using Satellite Imagery", Regional Conference on Geomatics for Good Governance 2011, Kashmir., 13-14 sep 2011.

[10] Singh, P., Polglase, L. and Wilson, D., 2009. Role of Snow and Glacier melt runoff modeling in Hydropower projects in the Himalayan Region. In (WEES -2009).

[11] Zhen Xiong and Yun Zhang, Bundle Adjustment With Rational Polynomial Camera Models Based on Generic Method, IEEE TGRS, VOL. 49, NO. 1, JANUARY 2011

[12] Jain, K., Ravibabu, M.V., Shafi, J.A. & Singh, S.P. (2009)-Using Rational Polynomial Coefficients -(RPC) to generate digital elevation models - a comparative study, Applied GIS, 5(2), 1-11.

[13] Kumar, R., G. Areendran and P. Rao. 2009. Witnessing change: glaciers in the Indian Himalayas. Pilani, WWF-India and Birla Institute of Technology.

[14] Dashora, A. and Lohani, B. and Malik J. N., 2007: A repository of earth resource information – CORONA satellite programme, in: Current Science, vol. 92, no. 7, pp. 926-932.

Fig 6: GPS Observation around Goumukh using Handheld Trimble GPS (14/10/2012)